A REVIEW OF PERFORMANCE PREDICTION METHODS FOR PUMP AS TURBINES

Eren GÜVEN
Mechanical Engineer & Electronics and Communication Engineer
Standart Pompa ve Makina San. Tic. A.Ş.
Istanbul, Turkey, erenguven@standartpompa.com

ABSTRACT

Pump as turbine (PAT) can be preferred for electricity generation in small and micro hydropower plants and drinking water supply networks in isolated areas. The main reasons to use PAT for this applications include low initial investment costs, ease of operation and maintenance, and short delivery times. The reliability of empirical methods used to predict PaT performance is a major problem in PAT selection. In this study, it is shown that PAT performance can be predicted by three-dimensional computational fluid dynamic (CFD) simulations as an alternative to empirical methods. For this purpose, an end suction pump, a double suction pump and a multistage pump were selected and their performances in turbine mode were measured experimentally. The alignment between numerical results and experimental measurements showed that CFD can be used successfully in PAT selection. Also, if numerical calculations can not be performed, the capabilities of empirical correlations in predicting PAT performance are discussed.

SYMBOLS

k_Q : Turbine flow conversion coefficient
k_H : Turbine head conversion coefficient
η : Efficiency
η_p : Pump efficiency
η_t : Turbine efficiency
Q_{opt} : Pump flow rate at best efficiency point(BEP) (m^3/h)
H_{opt} : Pump head rate at best efficiency point(BEP) (m)
n_q : Pump specific speed
Q_t : Turbine flow rate (m^3/h)
H_t : Turbine head (m)
P : Shaft Power (kW)

1.INTRODUCTION

The energy requirement of the world increases in proportion to the increasing population and demand. Regardless of whether the capacity of water resources is large or small, the high initial costs prevent investing in establishing electrical energy generation plants [1]. Therefore energy producers seek to reduce the unit cost, which increases research studies on micro hydroelectric power plants. It has been understood that PATs can be used as an alternative to conventional turbines to reduce the equipment cost of micro hydroelectric power plants.

PATs have different specific speeds, hydraulic structures and mechanical structures among each other. The most common types of PATs in practice are end suction pumps, double suction pumps and multistage pumps.

Pump manufacturers use performance prediction methods for PAT selection due to difficulties in achieving experiment results [2]. The performance prediction methods are related with specific speed of the pump, head and the flow rate at the best efficiency point of the pump. Coefficients of prediction methods are shown in Table 1.

Table 1 : PAT conversion formulas

	k_Q	k_H	η
Stephanoff [3]	$\frac{1}{\sqrt{\eta_p}}$	$\frac{1}{\eta_p}$	$\eta_t = \eta_p$
Childs [4]	$\frac{1}{\eta_p}$	$\frac{1}{\eta_p}$	$\eta_t = \eta_p$
Sharma [5]	$\frac{1}{\eta_p{}^{0,8}}$	$\frac{1}{\eta_p{}^{1,2}}$	$\eta_t = \eta_p$
Alatorre-Frenk [6]	$\frac{0,85\eta_p{}^2 + 0,385}{2\eta_p{}^{9,5} + 0,205}$	$\frac{1}{0,85\eta_p{}^2 + 0,385}$	$\eta_t = \eta_p - 0,03$
Yang [7]	$\frac{1,2}{\eta_p{}^{0,55}}$	$\frac{1,2}{\eta_p{}^{1,1}}$	$\eta_t = \eta_p$
NMHP [8]	1,25	1,38	$\eta_t = \eta_p$
Smit [9]	1,65	2	$\eta_t = \eta_p$

Flow rate and head of the PAT are calculated by formula (1) and formula (2) respectively. Chapallaz[10] stated that there is a deviation of more than 20% in the estimations made by these methods. Precision of these methods has a vital role on loss of money, time and labor which are caused by wrong predictions.

$$Q_t = k_Q.\, Q_{opt} \quad (1)$$
$$H_t = k_H.\, H_{opt} \quad (2)$$

In this research, PAT performances of these three different type of pumps with different specific speeds were analyzed numerically and empirically, and compared with PAT experiment results. The pump properties are shown in Table 2.

Table 2 : Capacity, head, efficiency, speed and specific speed of the pumps

Characteristics	PAT #1 End Suction	PAT #2 Double Suction	PAT #3 Multistage
Q_{opt}(m^3/h)	123	210	335
H_{opt}(m)	21,3	58	131
η_{opt}(%)	81,3	76,1	77,7
speed (rpm)	1800	1500	1500
n_q	33,56	12,19	26,94

2. EXPERIMENTAL SETUP

The general view of the experimental setup of PAT is given in Figure 1. PATs are tested in a closed-loop, 450 m^3 water tank. Magnetic flow meter is used to measure capacity at the discharge, power analyzers are used to measure electrical power from the turbine generator, input and output pressure transmitters are used to measure pressure values in the experiment.

The inlet of the turbine is supported with a booster pump to generate head. Generated electric is regulated to harness the energy.

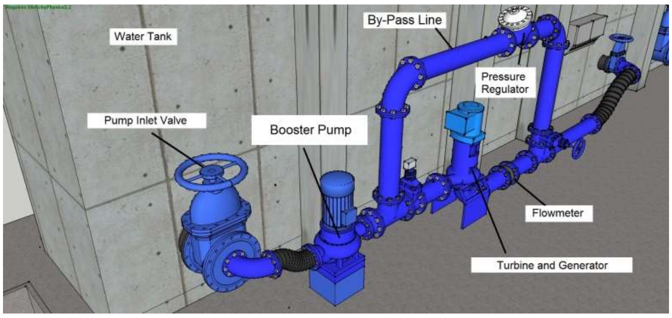

Figure 1 : View of the experimental setup of PAT [2]

3. NUMERICAL ANALYSIS

Detailed information regarding the generation of 3D flow volumes, meshing, calculation methods, velocity and pressure distributions are shown in the section 3.1 and 3.2.

3.1 GENERATION OF 3D VOLUMES AND MESH

The 3D flow volume is constructed using the surfaces of the model contacting the fluid. These models do not include casing cover for stuffing box, bearing housing and seals. After the flow volume is formed including volute casing and impeller, meshing is applied on the model [11].

FLUENT software was used for flow analysis. Incompressible Navier-Stokes equations are solved by the finite volume method, and the turbulence is modeled by the realizable k-ε method.

Mass flow inlet boundary condition is prescribed of PAT inlet and pressure outlet boundary condition is prescribed at the outlet. No-slip boundary condition is applied at the walls. Continuum domain is selected as cold water.

In the analysis, additional volumes have been placed to ensure a uniform flow profile at the inlets and outlets.Leakage flow does not include in the modelling due to increase calculation time. Leakage loss and mechanical loss were calculated using empirical formulas as given in the literature and used in the turbine efficiency calculation.

Mesh is generated with ANSYS MESH software. Number of elements for each PAT and area weighted average of y+ values on blade are in shown in Table 3.

Table 3: Mesh characteristics

	PAT #1	PAT #2	PAT #3
Number of elements	6930647	2642557	7428629
Area weighted average of y+ values on blade	139	325	440

Meshing views of the PATs are shown in Figure 2.

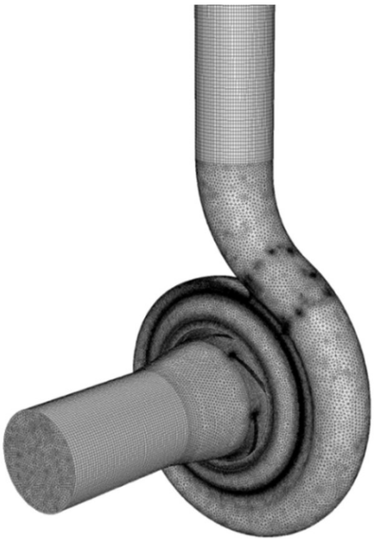

a)

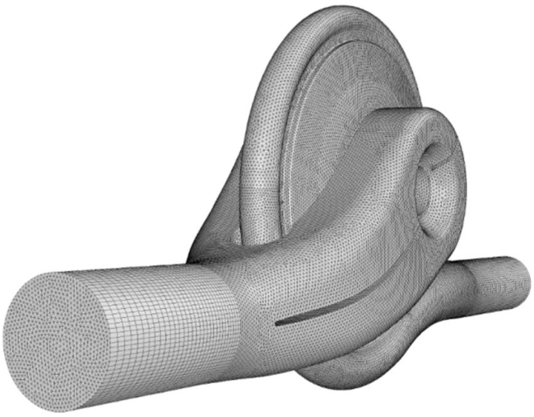

b)

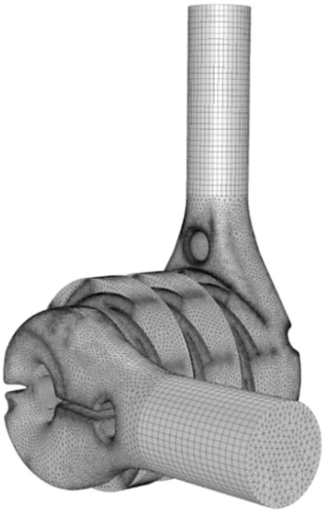

c)

Figure 2 : View of mesh a) PAT #1 b) PAT #2 c) PAT #3

3.2 NUMERICAL RESULTS

Convergence criteria is selected such that the residuals of continuity, momentum and turbulence drop below 10^{-4}. Calculations are be repeated for different flow rates.

In PAT design, the priority is to achieve the most efficient turbine with least changes on the pump design. Since hydraulic geometry is constructed for pump mode operation, flow separations and friction losses are inevitable in turbine mode.

Velocity and pressure distributions are examined for three different PATs at their BEP.

Velocity and pressure distributions of PAT #1 in meridional and radial sections at 156 m^3/h are shown in Figure 3. It is seen that flow separation mainly occur at the impeller. Flow is rather smooth in the volute casing. Blade inlet angle and angle distributions over the blade, which is designed for the pump, have great impact flow separations. Static pressure distribution shows that energy is absorbed from periphery to center.

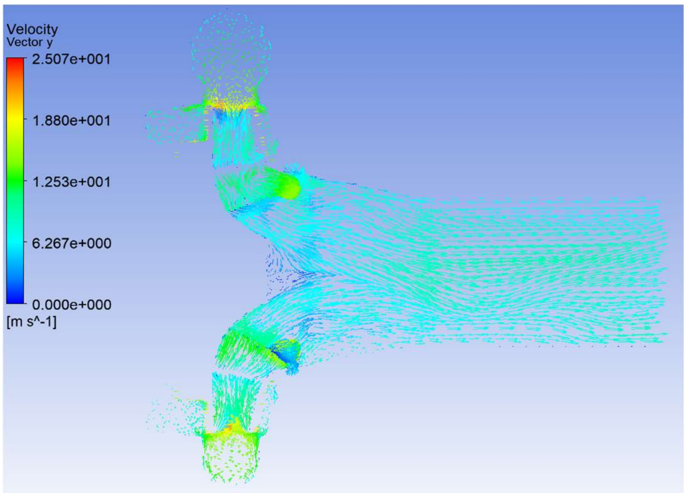

a) Velocity vectors in meridional view

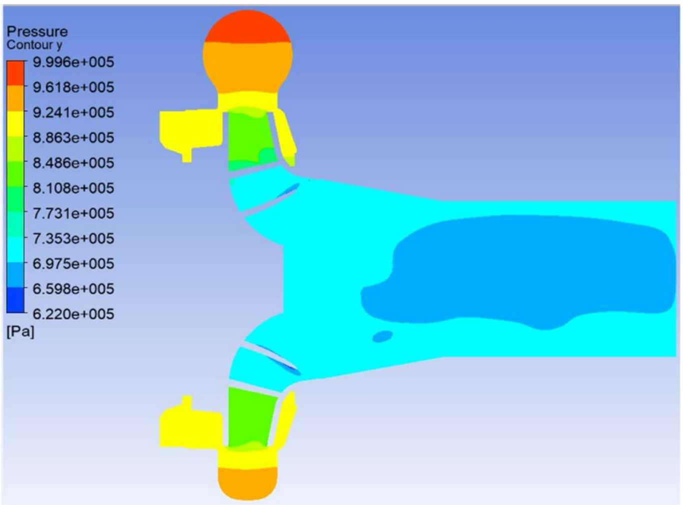

b) Pressure distribution in meridional view

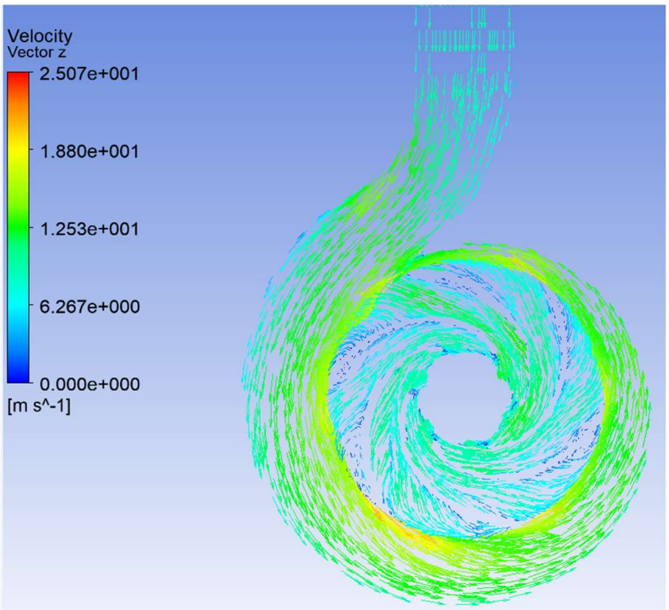

c) Velocity vectors in radial section

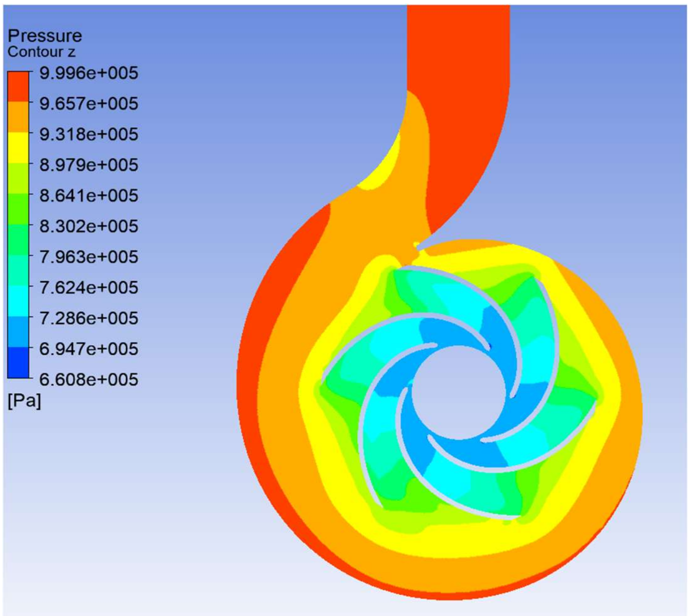

d) Pressure distribution in radial section

Figure 3: Velocity and pressure distributions of PAT #1 at 156 m^3/h

Velocity and pressure distributions of PAT #2 in meridional and radial sections at 250 m^3/h are shown in Figure 4. It is seen that the flow is quite uniform in the volute casing. On the other hand excessive deceleration is observed in the impeller passages. Static pressure distribution shows that energy is absorbed from periphery to center.

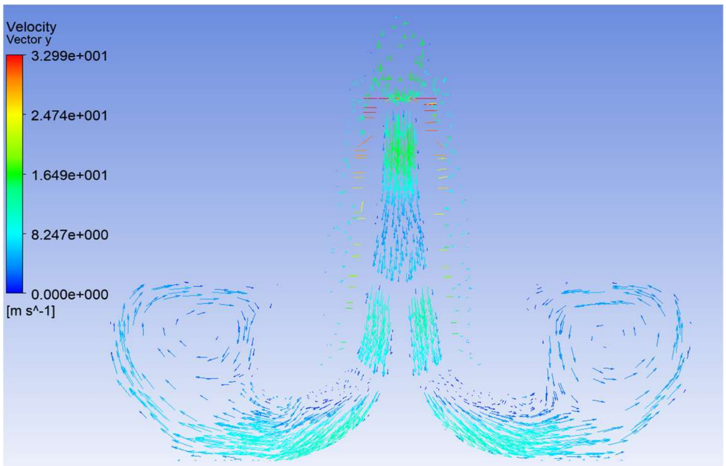

a) Velocity vectors in meridional view

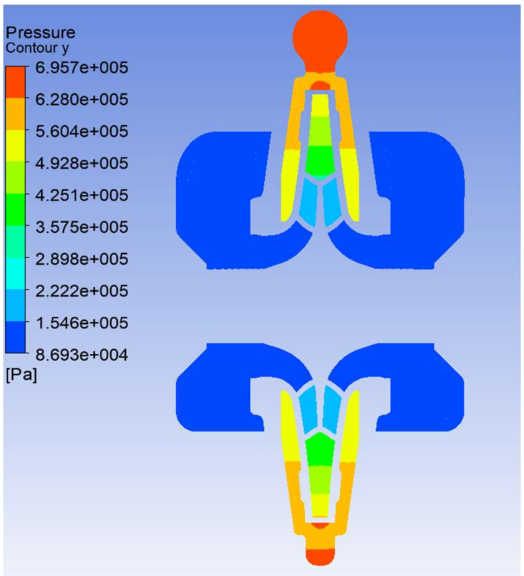

b) Pressure distribution in meridional view

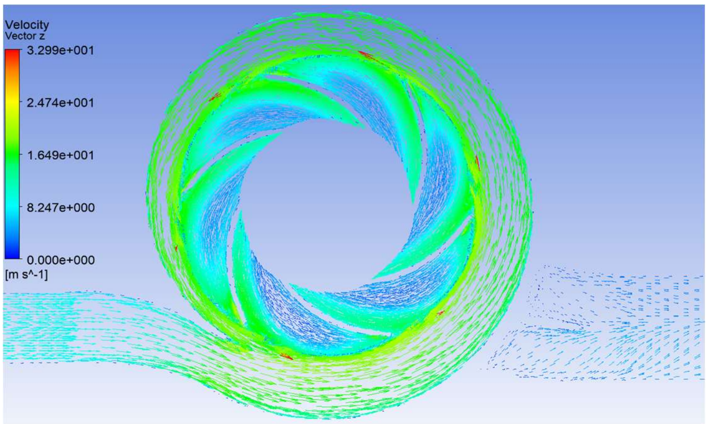

c) Velocity vectors in radial section

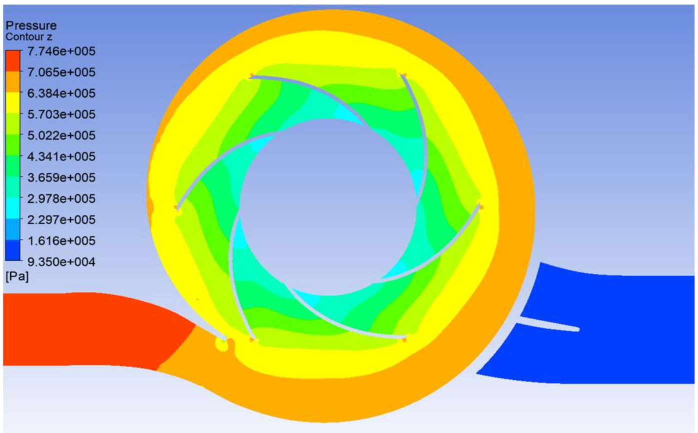

d) Pressure distribution in radial section

Figure 4: Velocity and pressure distributions of PAT #2 at 250 m^3/h

Velocity and pressure distributions of PAT #3 in meridional and radial sections at 570 m^3/h are shown in Figure 5. The result reveal that, unlike the other two PATs, impeller and diffuser blade angles suit well for turbine mode operation. In that sense no flow seperation is observed. An uniform pressure distribution along the tangential direction is achieved.

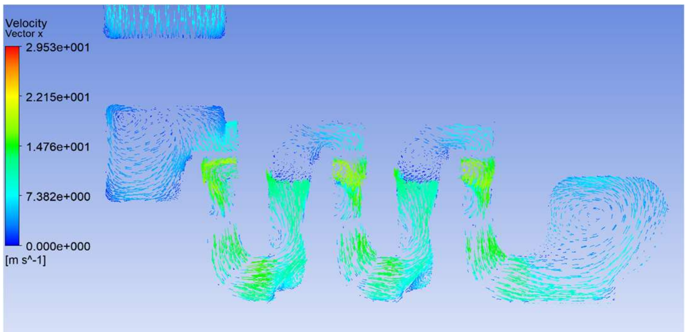

a) Velocity vectors in meridional view

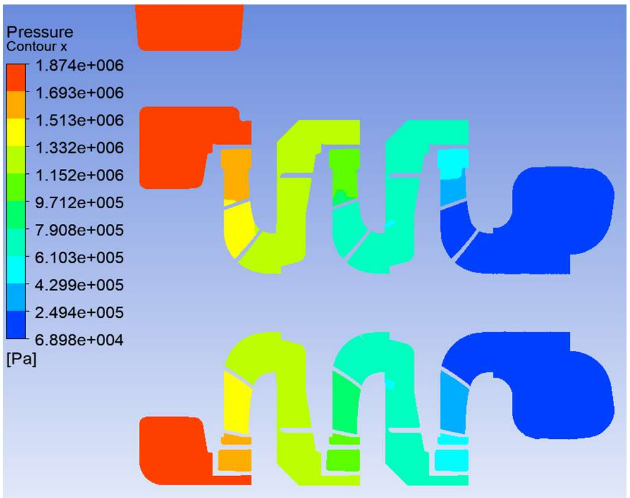

b) Pressure distribution in meridional view

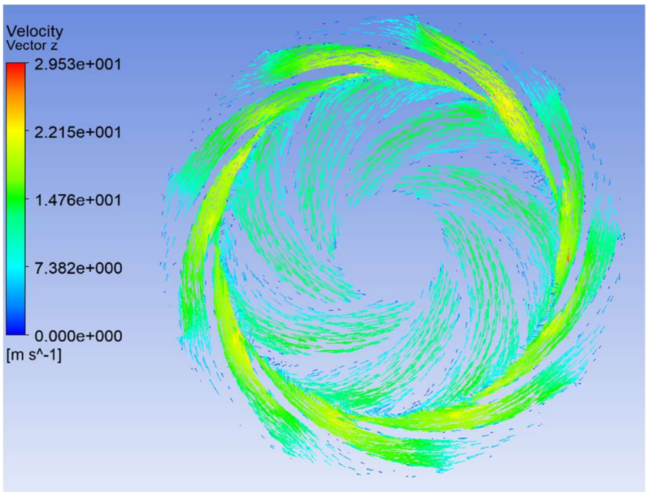

c) Velocity vectors in radial section

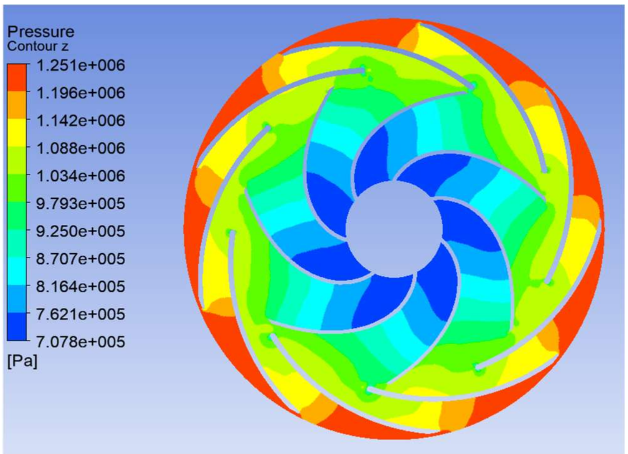

d) Pressure distribution in radial section

Figure 5: Velocity and pressure distributions of PAT #3 at 570 m^3/h

4. COMPARISON OF THE EXPERIMENTAL AND NUMERICAL PERFORMANCE CURVES

Accuracy of numerical H-Q and P-Q curves is compared with experimental results. Calculated leakage loss and mechanical loss by empirical formulas are used in the turbine efficiency calculation.

As shown in Figure 6, the CFD results have good accuracy predicting the experimental H-Q curve in PAT #1. A ≈ 10% difference is seen on the P-Q curve.

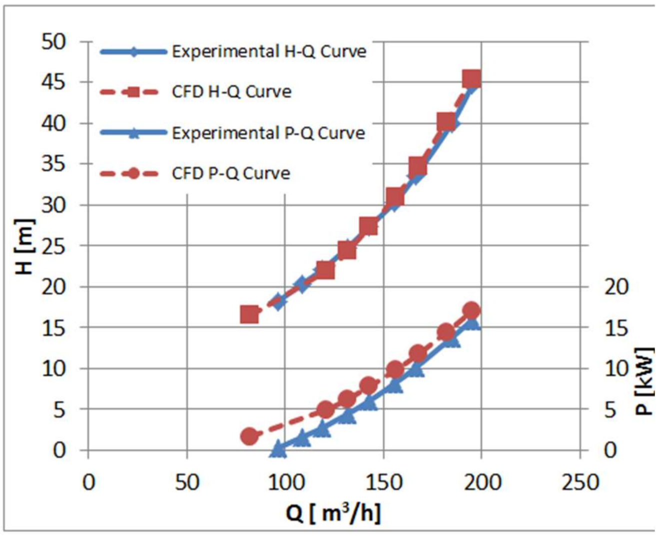

Figure 6: Comparison of CFD and experimental results of PAT#1

Experimental results of H-Q and P-Q curves of PAT #2 overlap with the numerical results as seen in Figure 7.

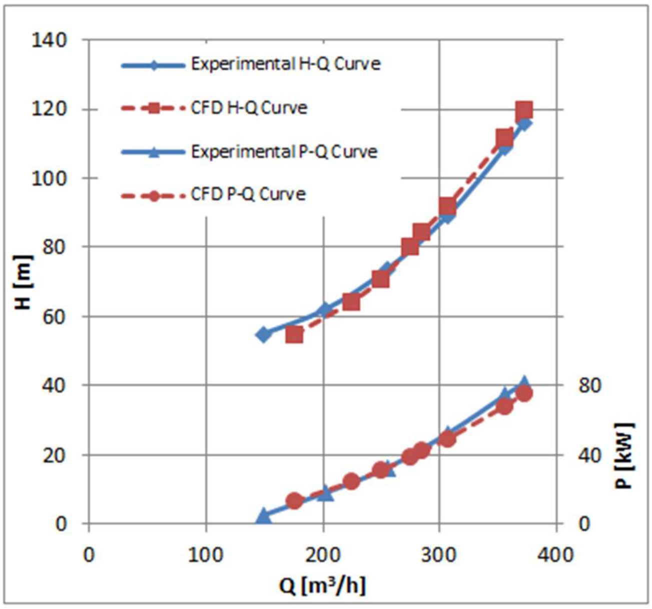

Figure 7: Comparison of CFD and experimental results of PAT#2

As it is seen in Figure 8, CFD results of PAT #3 has ≈ 7% deviation from the experimental results.

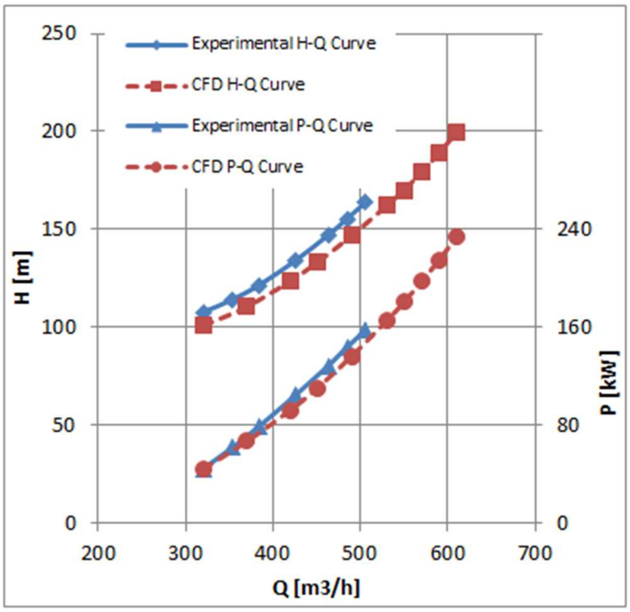

Figure 8: Comparison of CFD and experimental results of PAT#3

5. COMPARISON OF EXPERIMENTAL RESULT AND EMPIRICAL FORMULAS

PAT performances at the best efficiency point are compared with the empirical results from the literature.

As it is seen in Figure 9, predicted PAT performance points using empirical formulas for PAT #1 and #2 are consistent with experimental result, unlike PAT #3. Also, it should be noted that the empirical formulas can only yield the BEP at the PAT.

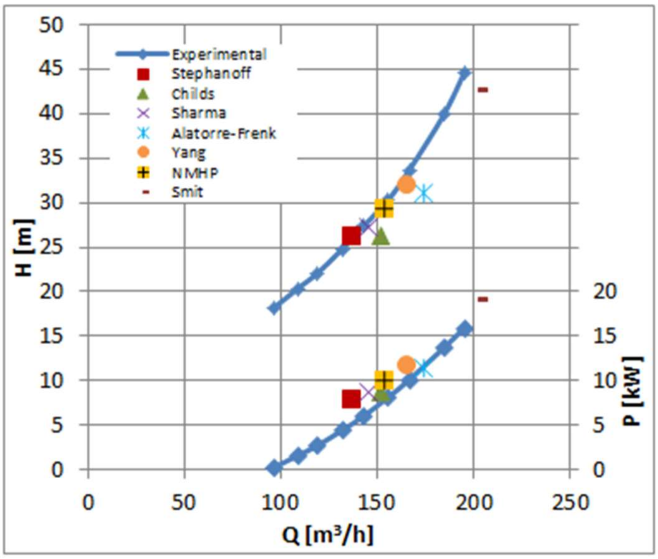

a)

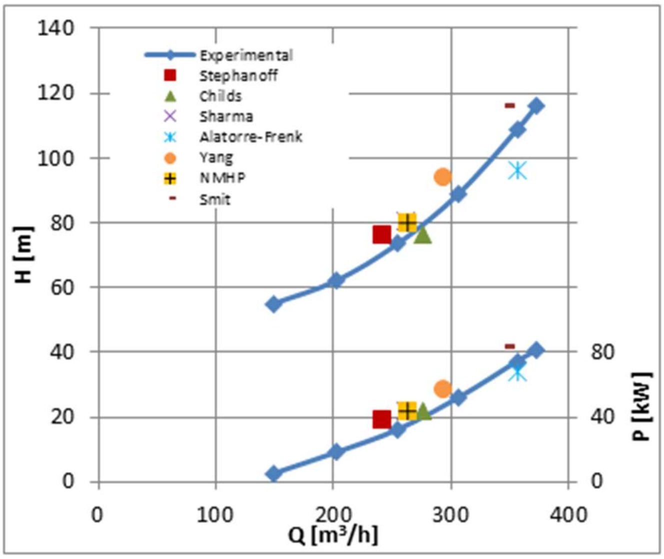

b)

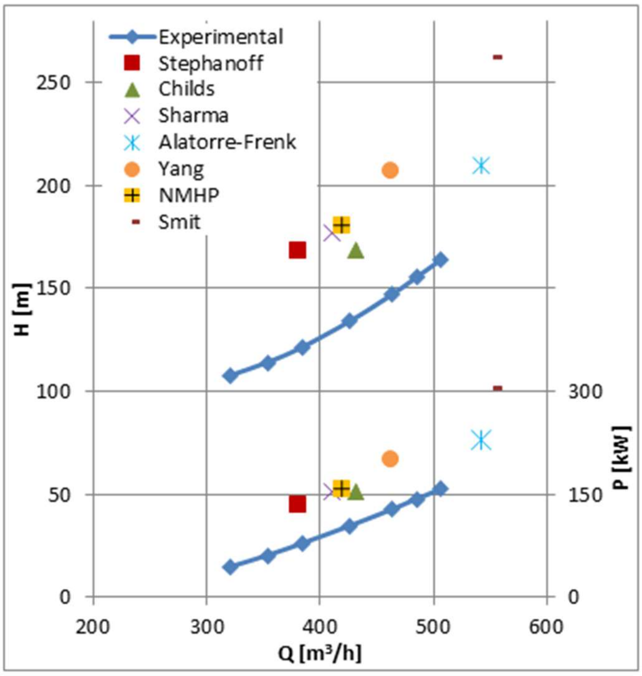

c)

Figure 9: Comparison of experimental results with empirical equations a) PAT #1 b) PAT #2 c) PAT #3

6. RESULTS

PAT performances were analyzed numerically and empirically by selecting three pumps including an end suction, a double suction and a multistage pump. Results were compared with PAT experiments. For all three PAT performance predictions, the numerical results were found to be consistent with the experiments.

Empirical formulas are found to be successful in predicting the BEP of PATs #1 and #2. This success could not be achieved in PAT #3. Therefore, it would not be right to generalize that the empirical relations are an absolutely reliable selection method. In addition, we can only estimate one point on the PAT performance curve with these methods.

It is considered that CFD simulations are necessary for a correct PAT selection. Nevertheless, it is seen that empirical relations can be used as an auxiliary tool for the selection of the PAT.

ACKNOWLEDGMENTS

I would like to thank to Cezmi Nurşen, R&D Manager of Standart Pompa, who provided to experimental results. I would like to extend my sincere thanks to Technical Designer Fuat Baskın, Prof. Dr. Haluk Erol, Dr. Mehmet Kaya and electrical engineers of the company.

REFERENCES

1.E.C. Nurşen, M. Yeğin, K.S. Yiğit, 2019, "Santrifüj Pompalarn Hidrolik Türbin Olarak Kullanılması"

2.E.C. Nurşen, K.S. Yiğit, Ö. Kaplan, 2019, "Kademeli Tip Santrifüj Pompaların Hidrolik Türbin Olarak Kullanılmasının Deneysel Olarak İncelenmesi"

3.A.J. Stepanoff, 1957, Centrifugal and Axial Flow Pumps: Theory, Design and Application; JohnWiley: New York, NY, USA.

4.S.M. Childs, 1962, Convert pumps to turbines and recover HP. Hydro Carbon Process. Pet. Refin. 41, 173–174.

5.K. Sharma, 1985, Small Hydroelectric Project-Use of Centrifugal Pumps as Turbines; Technical Report; Kirloskar Electric Co.: Bangalore, India.

6.C. Alatorre-Frenk, 1994, Cost Minimization in Micro Hydro Systems Using Pumps-as-Turbines. Ph.D. Thesis, University ofWarwick, Coventry, UK.

7.S.S. Yang, S. Derakhshan, F.Y. Kong, 2012, Theoretical, numerical and experimental prediction of pump as turbine performance, Renew. Energy 48 507-513.

8.Nepal Micro Hydro Power, 2005, Pump-as-turbine technology. Intermediate Technology Development Group. September 29

9.E.N. Smit, 2005, Micro Hydro Power Generation. Final Year Project Report. Faculty of Engineering, Stellenbosch University

10.J.M. Chapallaz, P. Eichenberger, G .Fischer, 1992, "Manual on pumps used as turbines. ", In Friedr Vieweg Sohn Verlagsgesellschaft, Braunschweig; Informatica International, Inc.: Braunschweig, Germany.

11.M. Kaya, 2009, "Santrifüj Pompa Performansının Sayısal Analizi", Master Thesis